Characterization of *TPM1* Disrupted Yeast Cells Indicates an Involvement of Tropomyosin in Directed Vesicular Transport

Haoping Liu and Anthony Bretscher

Section of Biochemistry, Molecular and Cell Biology, Biotechnology Building, Cornell University, Ithaca, New York 14853

Abstract. Disruption of the yeast tropomyosin gene *TPM1* results in the apparent loss of actin cables from the cytoskeleton (Liu, H., and A. Bretscher. 1989. *Cell.* 57:233–242). Here we show that *TPM1* disrupted cells grow slowly, show heterogeneity in cell size, have delocalized deposition of chitin, and mate poorly because of defects in both shmooing and cell fusion. The transit time of α-factor induced a-agglutinin secretion to the cell surface is longer than in isogenic wild-type strains, and some of the protein is mislocalized. Many of the *TPM1*-deleted cells contain abundant vesicles, similar in morphology to late secretory vesicles, but without an abnormal accumulation of intermediates in the delivery of either carboxypeptidase Y to the vacuole or invertase to the cell surface. Combinations of the *TPM1* disruption with *sec13* or *sec18* mutations, which affect early steps in the secretory pathway, block vesicle accumulation, while combinations with *sec1,sec4* or *sec6* mutations, which affect a late step in the secretory pathway, have no effect on the vesicle accumulation. The phenotype of the *TPM1* disrupted cells is very similar to that of a conditional mutation in the *MYO2* gene, which encodes a myosin-like protein (Johnston, G. C., J. A. Prendergast, and R. A. Singer. 1991. *J. Cell Biol.* 113:539–551). The *myo2-66* conditional mutation shows synthetic lethality with the *TPM1* disruption, indicating that the *MYO2* and *TPM1* gene products may be involved in the same, or parallel function. We conclude that tropomyosin, and by inference actin cables, may facilitate directed vesicular transport of components to the correct location on the cell surface.

TROPOMYOSIN has been found in many eucaryotes, including mammals, insects (Karlick and Fyrberg, 1986), nematodes, and recently the slime mold *Physarum* and the yeasts *Saccharomyces cerevisiae* and *Schizosaccharomyces pombe* (Liu and Bretcher, 1989*a*). In all cases tropomyosin has been found associated with actin filaments, although its function is only really understood in skeletal muscle.

Skeletal muscle tropomyosin is a rod-shaped coiled-coil dimer assembled from highly α-helical monomers. In striated muscle, tropomyosin dimers bind along the actin filament in a head-to-tail fashion, with each molecule spanning seven actin monomers. Associated with each tropomyosin dimer is a troponin complex; together the two protein complexes confer Ca^{2+} sensitivity on the acto-myosin interaction (Ebashi et al., 1969). Distinct tropomyosin subunits are expressed in smooth muscle cells, where they may also be involved in thin filament regulation (Cummins and Perry, 1974). Nonmuscle cells display an amazing heterogeneity in expression of tropomyosin isoforms, which results mainly from alternative splicing of transcripts from a small number of genes (Leesmiller and Helfman, 1991). The diversity and tissue-specificity of tropomyosin isoforms expressed in higher eucaryotes suggests that this protein may play an important role in the utilization of microfilaments for divergent cell-type specific functions. However, how tropomyosin does this remains to be elucidated.

The yeast *Saccharomyces cerevisiae* is an attractive system for studying a primitive cytoskeleton (Huffaker et al., 1987; Barnes et al., 1990; Solomon, 1991; Huffaker and Bretscher, 1991). It contains a single essential actin gene, designated *ACT1*, that encodes a protein with 88% sequence identity to actins from higher cells (Shortle et al., 1982; Ng and Abelson, 1980; Gallwitz and Sures, 1980). Actin shows a polarized distribution suggesting an involvement in oriented cell surface growth (Kilmartin and Adams, 1984; Adams and Pringle, 1984). At the beginning of the cell cycle, cortical actin patches with emanating cables are found at the site of bud emergence. As the bud grows, cortical patches are found enriched in the bud, and actin cables extend into the mother cell. Later in the cycle, cortical patches form around the bud neck and may be involved in cytokinesis. A number of studies indicate a role for the actin cytoskeleton in the determination of cell polarity, secretion, and localized surface growth. Novick and Botstein (1985) explored the phenotype of cells carrying the temperature sensitive actin alleles *act1-1* and *act1-2*. At the restrictive temperature the cells lost actin cables, the distribution of actin patches were less polarized, chitin deposition was delocalized, and the cells accumulated

Dr. Liu's current address is Whitehead Institute for Biomedical Research, Nine Cambridge Center, Cambridge, MA 02142.

both the secretory protein invertase and secretory vesicles. The phenotypic consequences of disruptions in genes encoding actin-binding proteins are beginning to be assessed. These include the genes for conventional myosin (encoded by *MYO1*; Watts et al., 1985, 1987), tropomyosin (*TPM1*; Liu and Bretscher, 1989*a*,*b*), profilin (*PFY1*; Magdolen et al., 1988; Haarer et al., 1990), capping protein (*CAP1*; Amatruda et al., 1990), fimbrin (*SAC6*; Adams and Botstein, 1989; Adams et al., 1989, 1991), and a 65-kD actin binding protein (*ABP1*; Drubin et al., 1988, 1990). Disruption of any of these genes is not lethal, but confers phenotypes of different severities. In preliminary studies of the *TPM1*, *PFY1* and *CAP1* gene disruptions, phenotypes similar to those of the conditional actin mutants were observed. In all cases, the actin cytoskeleton was altered, cells were larger and more spherical, and chitin deposition was abnormal, implicating the involvement of the actin cytoskeleton in cell polarity and cell wall synthesis. However, no detailed characterization of any of these mutants has appeared yet.

We have described the purification and characterization of a protein from *Saccharomyces cerevisiae* with properties characteristic of a tropomyosin. These properties, together with immunological cross-reaction to bovine brain tropomyosin and protein sequence and structural homology to tropomyosins from higher cells provided strong evidence for classifying the yeast protein as a tropomyosin (Liu and Bretscher, 1989*a*,*b*). In yeast, tropomyosin is found associated with the actin cables that extend from the daughter bud into the mother cell; it is not found associated with the cortical actin patches that localize mostly in the daughter cell and at the bud neck during cytokinesis. Tropomyosin is encoded by a single gene in yeast that contains no introns. In an earlier report we showed that elimination of this tropomyosin from yeast by gene replacement did not confer lethality, but resulted in slower growing cells with no detectable actin cables (Liu and Bretscher, 1989*b*). Since cells from which tropomyosin had been genetically eliminated are viable, a phenotypic comparison between the *TPM1* deleted and wild-type cells might uncover the function of tropomyosin in yeast, and shed light on the function of the actin cables. Here we present a detailed phenotypic characterization of yeast strains carrying a disruption of the *TPM1* gene.

Materials and Methods

Strains, Media, and Genetic Techniques

The genotypes of all yeast strains used in this paper are described in Table I. The *TPM1* gene was replaced by either the *URA3* or *LEU2* gene. The construction of the *tpm1Δ::URA3* has been described (Liu and Bretscher, 1989*b*). For the *LEU2* replacement, the *URA3* containing DNA fragment from the HindIII to the ScaI site in the *tpm1Δ::URA3/YIp352* plasmid was replaced by the *LEU2* gene of the HindIII-ScaI fragment from a YIp351 plasmid (Hill et al., 1986). This plasmid was linearized at the unique ScaI site and transformed into diploid yeast cells (ABY365). This results in the replacement of the DNA from −236 to +225 at the *TPM1* locus by *LEU2*. This replacement was confirmed by absence of detectable tropomyosin in Leu^+ segregants as determined by immunoblotting with antibodies to yeast tropomyosin (Liu and Bretscher, 1989*a*). *E. coli* strain DH5α was used for all bacterial manipulations. Yeast media and genetic techniques were used as described by Sherman et al. (1974). The LiAc method was used for all the yeast transformations (Ito et al., 1983).

Mating Assay

Two methods were used to measure the efficiency of diploid formation (Trueheart et al., 1987). (*1*) Quantitative mass mating. Haploid cells were grown in YEPD[1] (1% yeast extract, 2% peptone, 2% dextrose) medium at 30°C to no more than 5×10^6 cells/ml 2×10^6 a and α cells were mixed and filtered onto a sterile 25-mm HA filter (pore size 0.45 μm; Millipore Corp., Bedford, MA) (Dutcher and Hartwell, 1983). The filter was transferred onto a YEPD plate with the cells facing up. After 6 h incubation at 30°C, the cells were washed off the filter with sterile water, sonicated briefly to break up the clumps, and equal amounts of cells were plated on plates selective for diploid cells and YEPD plates for total cells. The ratio of diploid cells over the total number of cells gave the efficiency of diploid formation. (*2*) Micromanipulation of zygotes. Freshly grown a and α cells from YEPD plates were mixed and incubated on YEPD plates. After 4.5 h at 30°C, cells were spread on one side of a YEPD plate and zygotes were micromanipulated to a new area of the plate. Colonies arising from the zygotes were replica plated to test whether the zygotes had formed diploids or remained as haploids.

Invertase Assay

Cells were grown in YEP medium containing 5% glucose at room temperature to ~5×10^6 cells/ml, washed, and resuspended into YEP medium containing 0.1% of glucose at 37°C. At each time point, 10 ml of the culture was removed, the cells were pelleted and washed in 10 mM NaN_3. The cell wall was removed by incubating the cells in 0.1 ml of 1.4 M sorbitol, 25 mM potassium phosphate (pH 7.5), 25 mM β-mercaptoethanol, 5 mM NaN_3, 25 μg/ml Zymolyase (ICN ImmunoBiologicals, Lisle, IL) for 1 h at 37°C. The spheroplasts were pelleted, resuspended in 0.1 ml of 25 mM Tris-phosphate (pH 6.7), 1 mM DTT, 1 mM EDTA, and lysed by vortexing with glass beads. Cell debris was pelleted at 15,000 *g* for 2 min. Proteins from the periplasm and the spheroplasts were fractionated on a 5.5% polyacrylamide native gel and the gel was stained for invertase activity (Gabriel and Wang, 1969).

Fluorescence Microscopy

To visualize DNA, cells were stained with 1 μg/ml 4′, 6′-diamidino-2-phenylindole (DAPI) (Dutcher and Hartwell, 1983). Chitin was visualized after staining in 0.1% Calcofluor for 3 min and washing in distilled water (Sloat and Pringle, 1978). Actin was stained with rhodamine-phalloidin (Adams and Pringle, 1984). To localize a-agglutinin, a-agglutinin antiserum (Watzele et al., 1988), generously provided by Dr. W. Tanner, was used after preabsorption on *MATα* cells. MATa cells were grown in YEPD to ~2×10^6 cells/ml at room temperature. β-mercaptoethanol was added to the culture to final concentration of 1% and incubated for 1.5 h. This step reduces the background staining dramatically and also removes some constitutively expressed a-agglutinin from the cell wall seen in some strains. The cells were washed three times with YEPD medium and resuspended in fresh YEPD (pH 4) medium to recover for 30 min at room temperature. α-Factor was added to the culture to 10 μg/ml and cells were incubated at room temperature and at 37°C. At each time point, aliquots of α-factor induced cells were fixed by adding formaldehyde to 3.7% and incubated for 1 h. The fixed cells were washed with 10 mM Tris-HCl, 140 mM NaCl, 5 mM EDTA, pH 7.5, and labeled with a-agglutinin antibodies and then FITC-conjugated second antibodies in the same saline solution (Watzele et al., 1988).

Electron Microscopy

Cells were prepared for thin section electron microscopy as described (Walworth and Novick, 1987) and viewed in an electron microscope (model EM301; Philips Electronic Instrs. Co., Mahwah, NJ) operating at 80 kV.

Results

Disruption of the TPM1 Gene Reduces the Growth Rate and Alters Cell Morphology

Disruption of the *TPM1* gene resulted in a reduced growth rate. The doubling time of haploids harboring the *TPM1* gene disruption (*tpm1Δ*) at 30°C in rich media was ~140 min, whereas the doubling time for the corresponding *TPM1*$^+$

1. *Abbreviations used in this paper*: CPY, carboxypeptidase Y; YEPD, 1% yeast extract, 2% peptone, 2% dextrose.

Table I. Yeast Strains Used in This Study

Strains	Genotype	Source
CUY25	*MATa ade2 his3-Δ200 leu2-3,112 ura3-52*	T. Huffaker
CUY28	*MATα his3-Δ200 leu2-3,112 lys2-801 trp1-1(am), ura3-52*	T. Huffaker
CUY29	*MATa his3-Δ200 leu2-3,112 lys2-801 ura3-52 GAL⁺*	T. Huffaker
ABY320	*MATα ade2 his3-Δ200 leu2-3,112 ura3-52 tpm1Δ::LEU2*	This study
ABY321	*MATa his3-Δ200 leu2-3,112 lys2 ura3-52 tpm1Δ::LEU2*	This study
ABY179	*MATa his4-539am ura3-52 tpm1Δ::URA3*	This study
ABY365	CUY25 × CUY28	
ABY366	ABY320 × ABY321	
DBY2000	*MATα act1-3 ura3-52*	A. Adams
CGY339	*MATα pep4 his4-29 ura3-52 GAL⁺*	CSH*
NY3	*MATa ura3-52 sec1-1*	P. Novick
NY10	*MATα ura3-52*	P. Novick
NY13	*MATa ura3-52*	P. Novick
NY17	*MATa ura3-52 sec6-4*	P. Novick
NY405	*MATa ura3-52 sec4-8*	P. Novick
NY414	*MATa ura3-52 sec13-1*	P. Novick
NY430	*MATa ura3-52 sec14-3*	P. Novick
NY431	*MATa ura3-52 sec18-1*	P. Novick
ABY409	*MATa ura3-52 sec1 tpm1Δ::URA3*	This study
ABY410	*MATα ura3-52 tpm1Δ::URA3*	This study
ABY411	*MATa ura3-52 tpm1Δ::URA3*	This study
ABY412	*MATa ura3-52 sec6-4 tpm1Δ::URA3*	This study
ABY413	*MATa ura3-52 sec14-3 tpm1Δ::URA3*	This study
ABY414	*ura3-52 sec4-3 tpm1Δ::URA3*	This study
ABY415	*ura3-52 sec13-1 tpm1Δ::URA3*	This study
ABY416	*ura3-52 sec18-1 tpm1Δ::URA3*	This study
JP7A	*MATα ade1 his6 leu2-3,112 ura3-52 myo2-66*	G. Johnston
JP7B	*MATa ade1 his3-Δ1 leu2-3,112 trp1-289 ura3-52 myo2-66*	G. Johnston
ABY100	*MATα his3-Δ200 leu2-3,122 lys2-801 ura3-52 ade2 tpm1Δ::LEU2 (TPM1 URA3)*‡	This study

* Obtained by A. Bretscher at the Cold Spring Harbor Laboratory course in yeast genetics.
‡ Genes listed in parentheses are carried on an autonomously replicating 2 μ plasmid.

haploids was 80 min. The slower growth of the *tpm1Δ* cells was not because of the death of a proportion of the cell population, since total cell and viable counts matched closely for both wild type and *tpm1Δ* cells (Fig. 1 *A*). However, at elevated temperatures the *tpm1Δ* cells hardly grew and were temperature-sensitive, with ~20% cell survival after 6 h at 37°C (Fig. 1 *B*). On plates, this temperature sensitivity was not very tight and varied with strain backgrounds. The *tpm1Δ* cells invariably reached stationary phase at a lower cell density than wild-type cells.

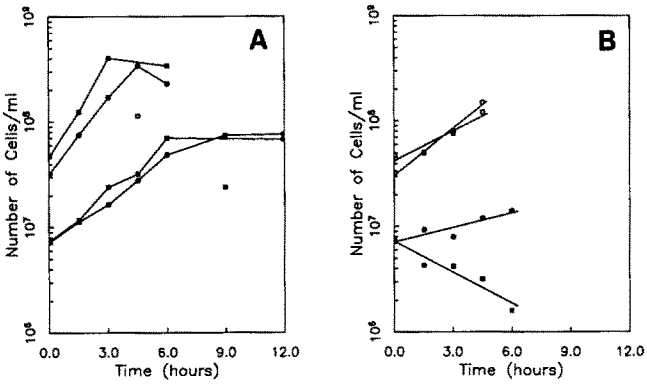

Figure 1. Growth and viability of *tpm1Δ* of *tpm1Δ* cells. Haploid wild-type (CUY25) and *tpm1Δ* cells (ABY321) were grown in YEPD at 30°C (*A*) or after shifting to 37°C (*B*) and the cells/ml was determined directly by counting, and the viable counts were determined after plating aliquots on YEPD plates. Wild-type cell counts (○), viable counts (□); *tpm1Δ* cell counts (●), viable counts (■).

Disruption of the *TPM1* gene is known to alter cell morphology and eliminate detectable actin cables from exponentially growing cells (Liu and Bretscher, 1989*b*). *tpm1Δ* cells were more spherical in shape and more heterogeneous in cell size than wild type controls, with many larger but also some smaller cells (Fig. 2, *A* and *B*). This phenotype was more severe in *tpm1Δ/tpm1Δ* diploid cells. DNA staining revealed that most of the mutant cells contained only one nucleus like wild-type cells; however, multiple nuclei were observed in some of the larger cells (Fig. 2, *C* and *D*). In agreement with the nuclear staining pattern, data from DNA content analyses showed that 6% of the *tpm1Δ/tpm1Δ* cells were tetraploid at 30°C, and the percentage of tetraploids increased after shifting the cells to 37°C for 5 h (data not shown). A small percentage of aploid cells was also seen at 37°C. This result, together with the cell size heterogeneity, suggests that *tpm1Δ* cells are partially defective in polarized cell growth, giving rise to smaller than normal daughter cells and larger than normal mother cells.

TPM1 disrupted cells generate petites at a much higher frequency than wild-type cells. More than 50% of the cells in a *tpm1Δ* culture grown in YEPD that were derived from a single ρ^+ colony were ρ^-, whereas only ~10% of the iso-

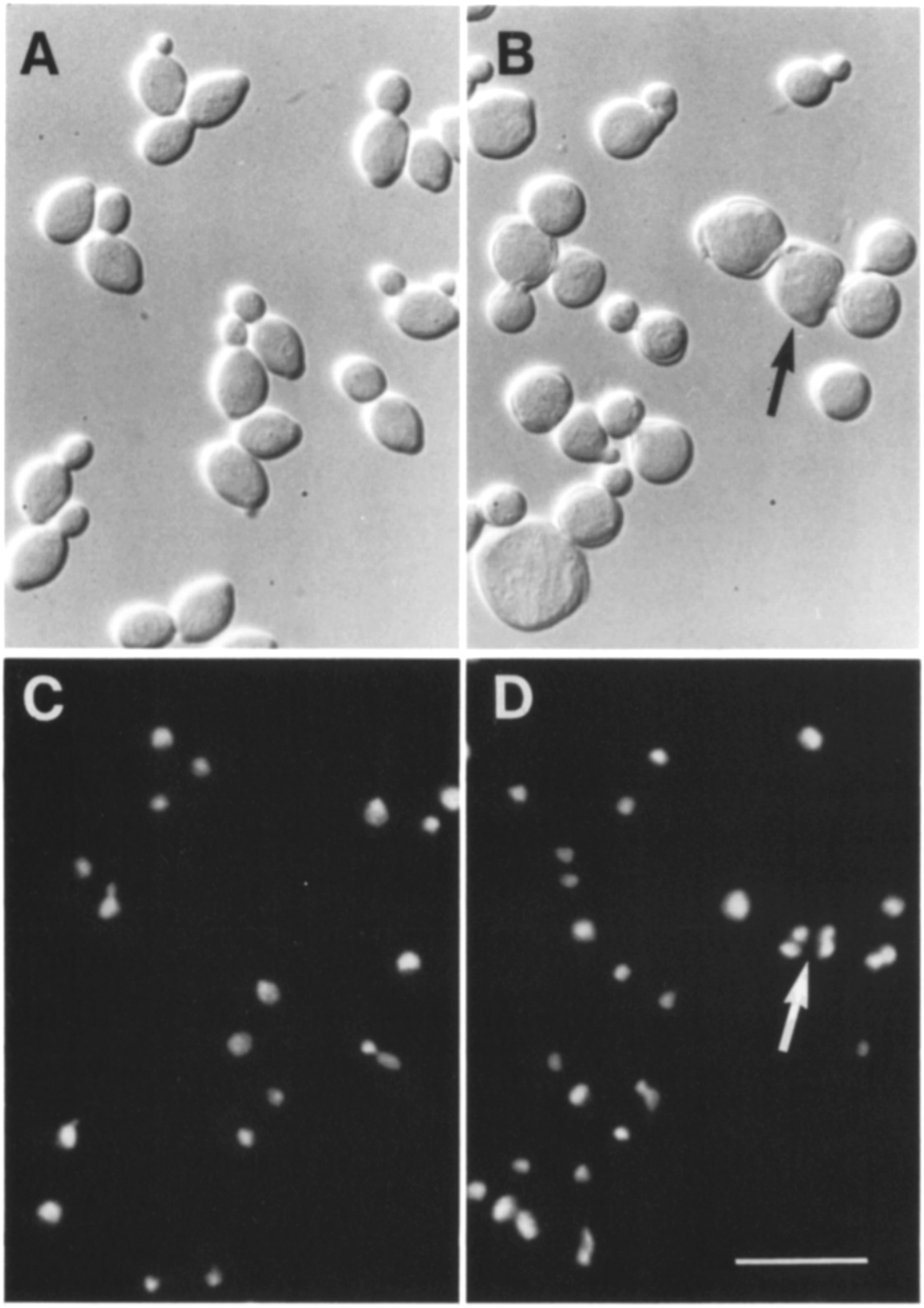

Figure 2. Morphology of wild-type (ABY365) and *tpm1Δ* diploid cells (ABY366). Wild type diploid cells (*A* and *C*) and *tpm1Δ* diploid cells (*B* and *D*) viewed by Nomarski optics (*A* and *B*) or after staining the DNA with DAPI (*C* and *D*) after growth at 30°C. Arrows in *B* and *C* indicate a cell containing four nuclei. Bar, 15 μm.

genic wild-type cells became ρ^- under the same conditions. This caused heterogeneity in colony formation of tropomyosin deficient cells as colonies derived from a ρ^+ cell had an uneven edge, surface, and size, whereas those from ρ^- cells were smaller, smooth, and uniform.

Disruption of the TPM1 Gene Impairs Cell Mating

Since *tpm1Δ* cells lack actin cables and are more spherical than wild-type cells, actin cables may be responsible for the generation of the asymmetric shape. The most dramatic

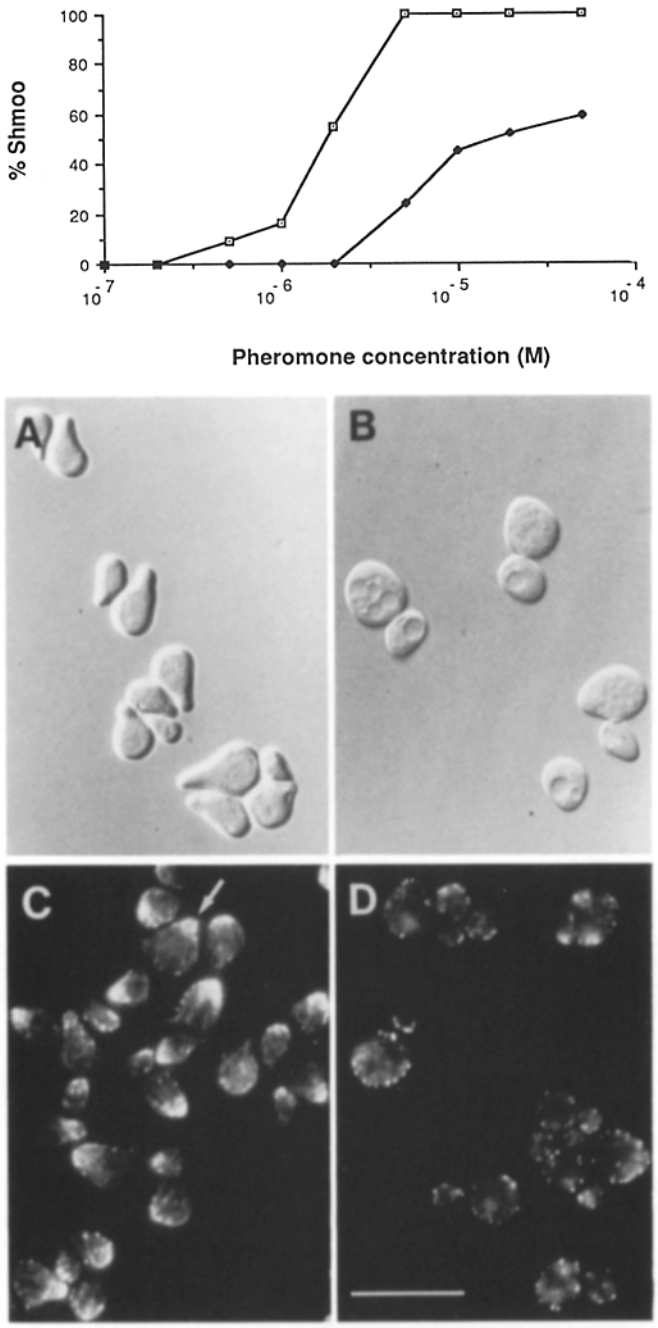

Figure 3. Response of wild-type (CUY25) and *tpml Δ* cells (ABY-320) to α-factor. (*Upper*) Dose response curves to wild type (□) and *tpml Δ* (♦) cells to α-factor. Cells were grown to 3 × 10^6/ml in YEPD (pH 4) at 30°C, treated with the indicated amount of α-factor for 3 h, fixed, sonicated, and counted under a microscope. Unbudded cells with one or more projections were counted as shmoo cells. (*Lower*) Morphology (*A* and *B*) and actin distribution (*C* and *D*) of wild-type (*A* and *C*) and *tpml Δ* cells (*B* and *D*) after 3 h of treatment with 10^{-5} M α-factor. Arrow in *C* indicates rearranged actin filaments during the formation of a second shmoo tip. Bar, 15 μm.

shape change in yeast cells occurs during mating, when cells of opposite mating types respond to mating pheromones by shmooing. To assess the ability of wild type and *tpml Δ* cells to shmoo in response to α-factor, *MATa* cells were incubated with various concentrations of the mating pheromone and the induced shmoo formation was scored. The resulting dose-response curves (Fig. 3) show that *tpml Δ* cells required ~5–10 times higher concentrations of α-factor to shmoo than the wild-type cells. Upon treatment with α-factor, *tpml Δ* cells became larger and arrested in the unbudded portion (G1) of the cell cycle. However, even at α-factor concentrations 10 times higher than required to induce shmoos in all wild-type cells, <60% of the *tpml Δ* cells had recognizable shmoo projections. In addition to this lower pheromone sensitivity, the *tpml Δ* shmooing cells formed less pronounced, thicker projection tips (Fig. 3 *B*). Longer exposure of the cells to α-factor gave similar results.

Cortical actin patches have been found concentrated at the shmoo tip of wild-type cells with actin cables extending into the body of the cell (Hasek et al., 1987). Actin cables are clearly evident in the shmoo neck of the wild-type cells, but were not seen in the *tpml Δ* cells (Fig. 3, *C* and *D*). In wild-type cells incubated longer with the pheromone, actin cables disappeared from the first shmoo tip and were reorganized to form dots and cables at a second shmoo tip (Fig. 3 *C*). After an extended period in α-factor, no actin cables and cortical patches were seen in the shmooing cells (not shown). This indicates that actin cables might be responsible for shmoo shape formation.

In addition to a defect in shmooing, *tpml Δ* cells showed a partial defect in cellular fusion during zygote formation. When cells of opposite mating types were mated on rich media, most of the zygotes formed between mating *tpml Δ* cells had a phase-dense plate between the mating partners, which was not seen in zygotes of isogenic wild-type cells (Fig. 4). The plate seen in the *tpml Δ* mating pairs is similar to that of *fus1fus2* prezygotes (Trueheart et al., 1987) and DNA staining of the *tpml Δ* prezygotes showed that the two nuclei had not fused. After extended mating (13 h) the nuclei in many of the *tpml Δ* prezygotic pairs had migrated to either side of the plate but were unable to fuse. This suggests a partial defect in cell fusion, rather than nuclear migration. To measure the magnitude of this defect in fusion, individual zygotes were picked by micromanipulation and the percentage giving rise to diploids was determined (Table II). About half of the zygotes from matings between *tpml Δ* cells failed to form diploids, and also a higher percentage failed to form viable colonies. These results suggest that the mating pairs derived from *tpml Δ* cells fail to fuse about half the time.

The combined defects in shmooing and cellular fusion lead to a much lower frequency of diploid formation. This was assayed in mass matings on nitrocellulose filters (Table III). In relation to the frequencies observed for matings between wild-type cells, crosses between *tpml Δ* and *TPM1*$^+$ cells reduced the formation of diploids by 80%, and between *tpml Δ* and *tpml Δ* cells by 98%. In addition, *tpml Δ/tpml Δ* diploids that were able to form, sporulate very poorly.

Disruption of the TPM1 Gene Causes Delocalized Chitin Deposition

A ring of chitin is formed at the neck of a budding cell and remains on the mother as a bud scar after cell division. In haploid cells the site of bud emergence is adjacent to the previous bud emergence site. Chitin rings provide a record of the site of earlier budding cycles. Strains carrying condi-

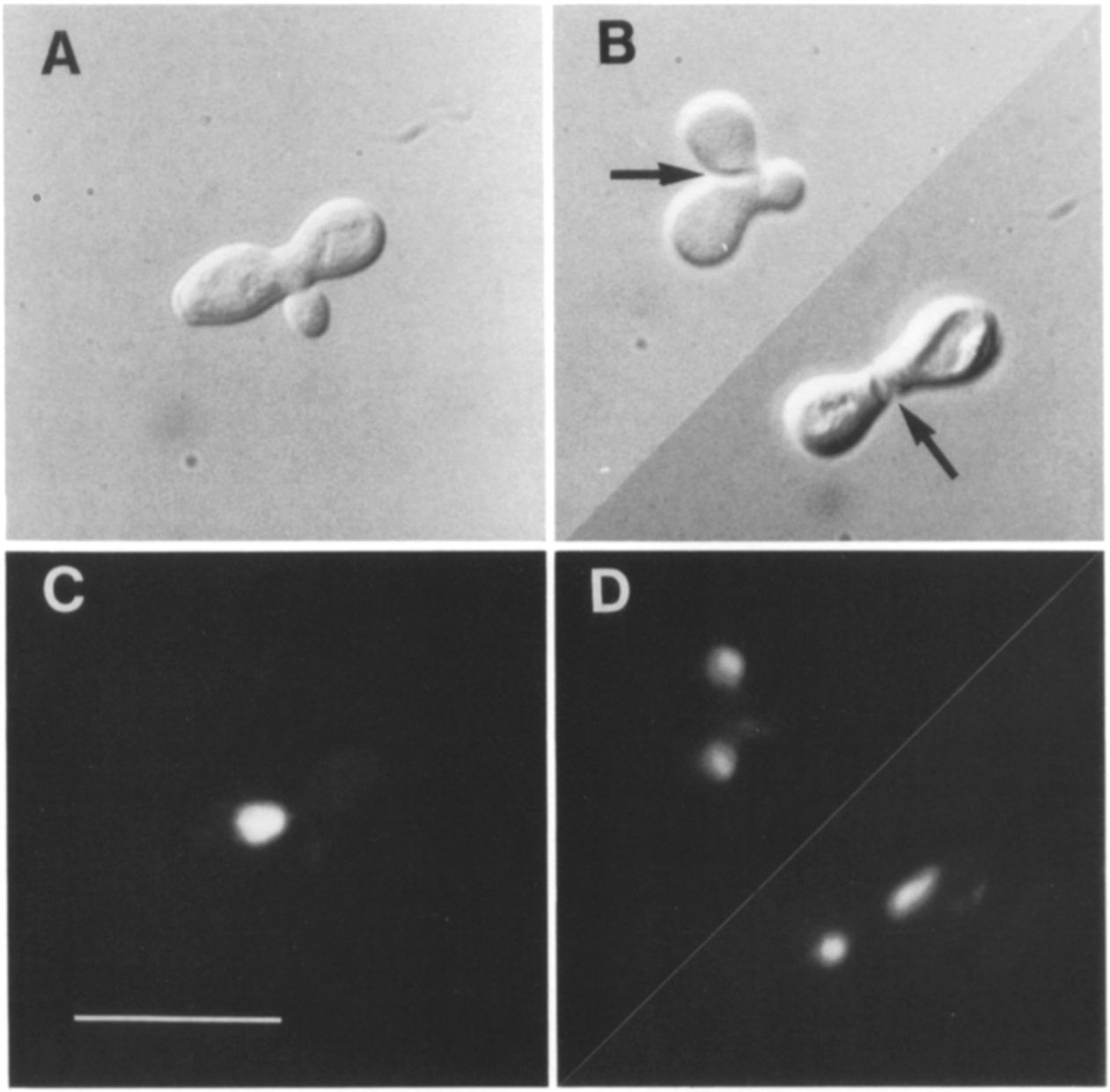

Figure 4. Morphology (*A* and *B*) and DNA localization (*C* and *D*) of conjugating cells. (*A* and *C*) *TPM1*$^+$ × *TPM1*$^+$ (CUY28 × CUY25); (*B* and *D*) tpm1Δ × tpm1Δ (ABY320 × ABY321) after 4.5 h at 30°C. Cells were photographed under Nomarski optics (*A* and *B*) or after staining with DAPI (*C* and *D*). Arrows indicate the phase dense plate between mating partners. Bar, 15 μm.

tional actin mutations and grown at the permissive temperature have large chitin rings and a general delocalized staining, and at the restrictive temperature they have bright staining over most of the cell (Novick and Botstein, 1985).

Table II. Diploid Formation in Micromanipulated Zygotes

Strains crossed	Diploids formed*
	%
a TPM1 (CUY25) × α *TPM1* (CUY28)	100 (39)
a TPM1 (CUY29) × α *tpm1Δ* (ABY320)	91 (36)
a tpm1Δ (ABY321) × α *tpm1Δ* (ABY320)	46 (27)

* The percentage of diploids among the colonies that grew from the micromanipulated zygotes (the actual number of the colonies that grew is shown in parentheses). In each cross, 48 zygotes were picked after cells of opposite mating types were mixed for 4.5 h at 30°C.

Localization of chitin in *tpm1Δ* cells at room temperature and at 37°C revealed similarities to the actin conditional mutants (Fig. 5). At room temperature, diffuse chitin rings and generalized overall staining was seen in *tpm1Δ* cells. The staining was quite heterogeneous and seemed to correlate

Table III. Efficiency of Diploid Formation in Crosses with tpm1Δ Cells

Strains crossed	Diploids formed
	%
a TPM1 (CUY25) × α *TPM1* (CUY28)	49
a tpm1Δ (ABY179) × α *TPM1* (CUY28)	10
a tpm1Δ (ABY321) × α *tpm1Δ* (ABY320)	0.6

The numbers are the percentage of diploids formed after 6 h at 30°C.

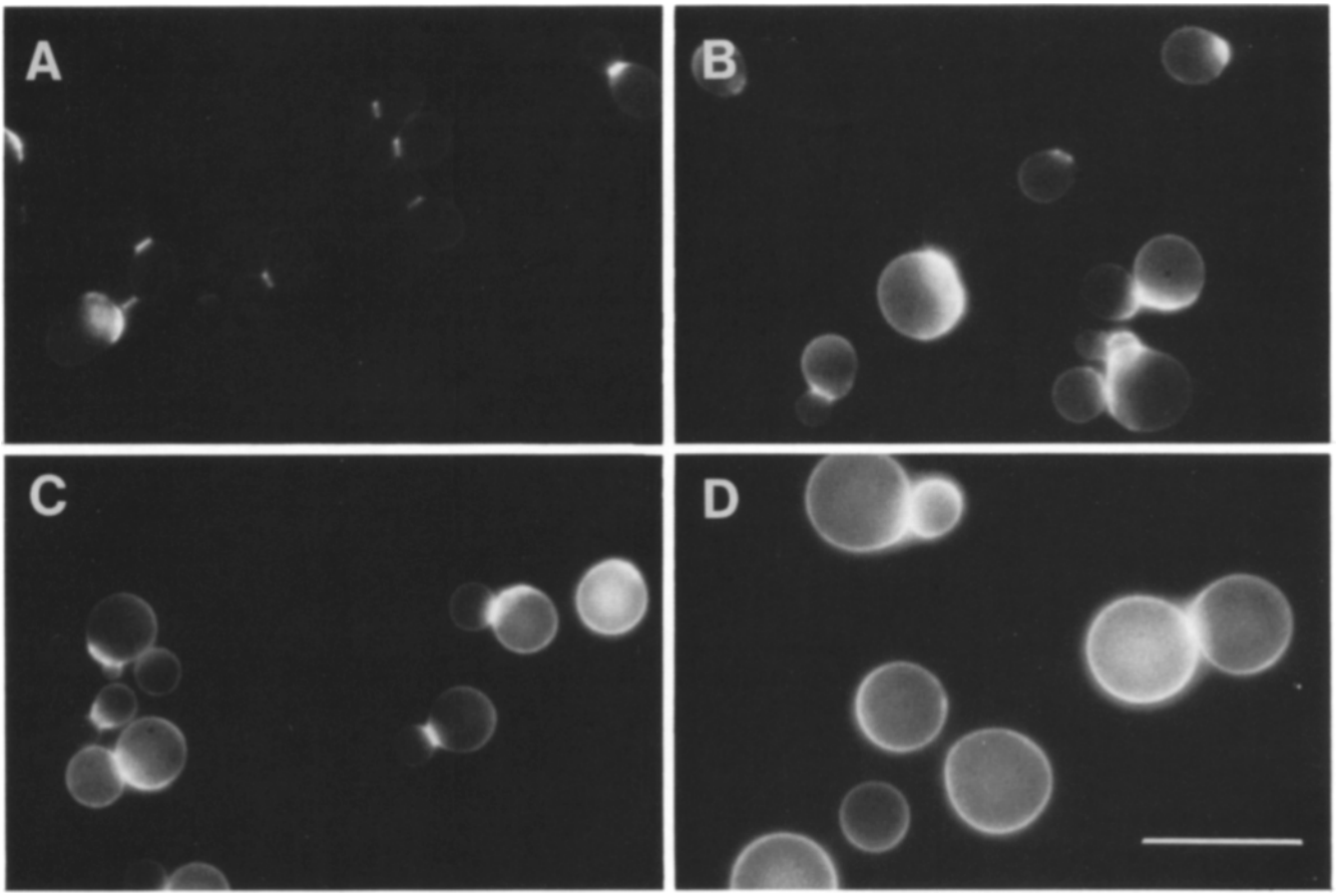

Figure 5. Chitin localization. Cells were grown to log phase and stained for chitin with calcofluor. (*A*) Wild-type cells (CUY25) grown at room temperature; (*B*) *act1-3* cells (CBY2000) grown at room temperature; (*C*) *tpm1Δ* cells (ABY320) at room temperature; (*D*) *tpm1Δ* cells after shifting to 37°C for 2.5 h. Bar, 15 μm.

with cell size, with larger cells having more delocalized staining. At 37°C, the staining was bright and mostly delocalized.

Disruption of the TPM1 Gene Affects Polarized Secretion of a-Agglutinin

Secretion and deposition of newly synthesized cell wall components in wild-type cells is directed to the growing buds in a process suggested to involve actin cables (Kilmartin and Adams, 1984; Adams and Pringle, 1984). Since the mechanism of chitin ring formation is not known, chitin deposition cannot be used to probe the behavior of the secretory and targeting pathways. A method of negatively staining with FITC-concanavalin A was used to localize the area of newly synthesized mannoproteins (Adams and Pringle, 1984). In this method, cells are labeled with FITC-ConA, chased in unlabeled growth medium for 30 min, and the unlabeled halo is used as an indication of the site of new cell wall deposition. Using this assay, bud growth in *tpm1Δ* cells seemed normal. However, since this method does not allow the detection of newly synthesized materials that are incorporated into preexisting cell walls, it can not reveal a partial defect in targeting. To detect any defects in localized secretion, the appearance of a-agglutinin at the cell surface was studied.

a-Agglutinin is an α-factor inducible cell surface glycoprotein in *MATa* cells. Upon α-factor treatment of exponentially growing *MATa* cells, the protein is first secreted exclusively to the growing bud and later to the tip of the pear-shaped shmoo (Watzele et al., 1988). a-Agglutinin was localized by immunofluorescence microscopy in *tpm1Δ* and wild-type cells at various times after α-factor addition (Fig. 6). At room temperature, the localization was similar in the two strains with a-agglutinin appearing at the cell surface 30 min after induction and concentrated in the buds (Fig. 6, *A* and *B*). At 180 min the staining was observed at the tips of the shmooing cells. However, the staining pattern of wild type and *tpm1Δ* cells at 37°C was different. a-Agglutinin was seen on the cell surface of wild type but not *tpm1Δ* cells at 30 min, and scattered patches appeared on the surface of the mother *tpm1Δ* cells at 60 and 90 min after induction, although staining in most cells was concentrated in the buds.

Disruption of the TPM1 Gene Does Not Block Secretion

The delayed appearance and partial delocalized incorporation of a-agglutinin on the cell surface could indicate an impairment in the secretory pathway. The status of the secretory pathway was assessed by examining the secretion of the periplasmic enzyme invertase and the delivery of a vacuolar enzyme carboxypeptidase Y (CPY).

Invertase is the product of the *SUC2* gene, which encodes

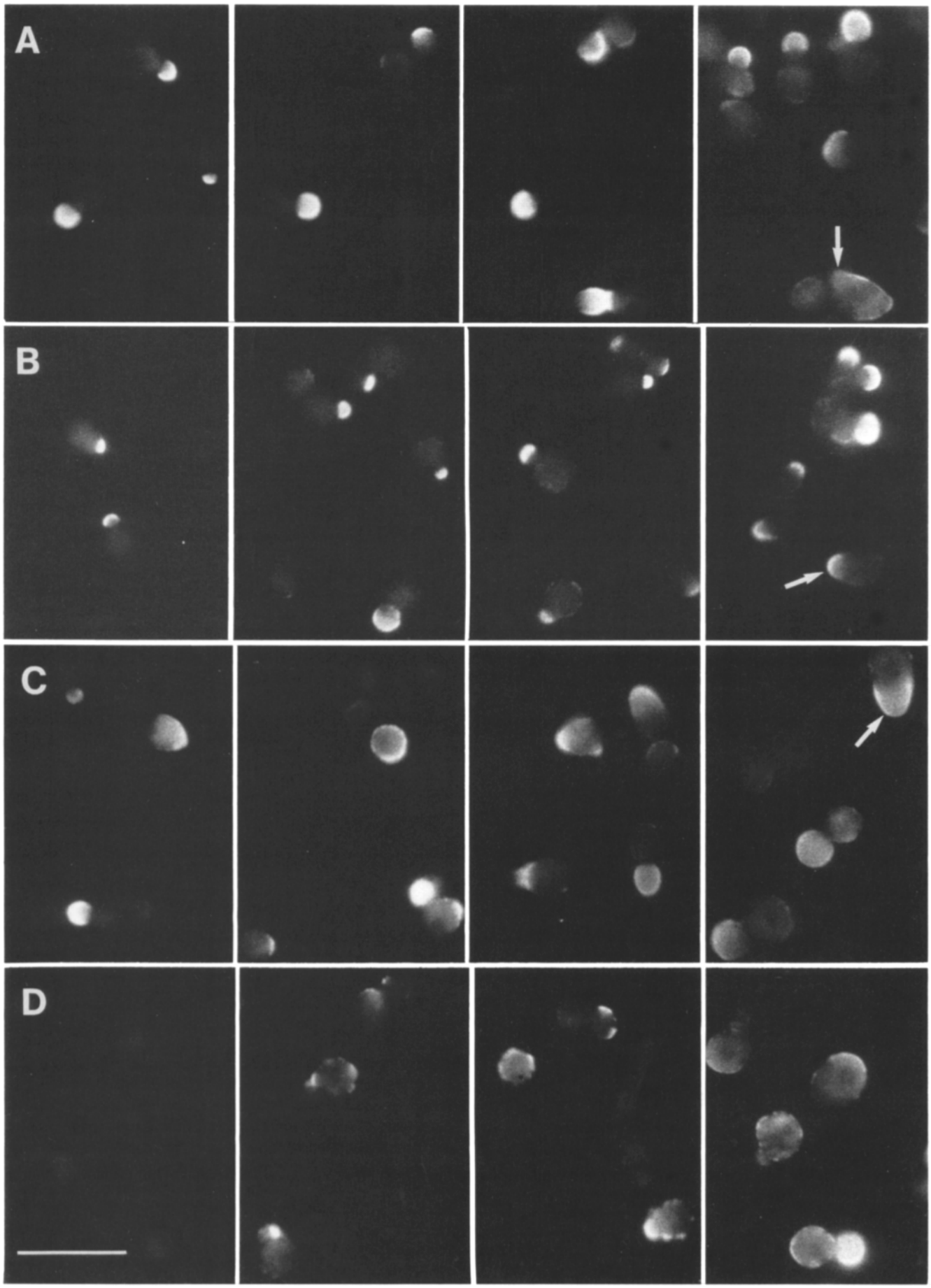
A
B
C
D

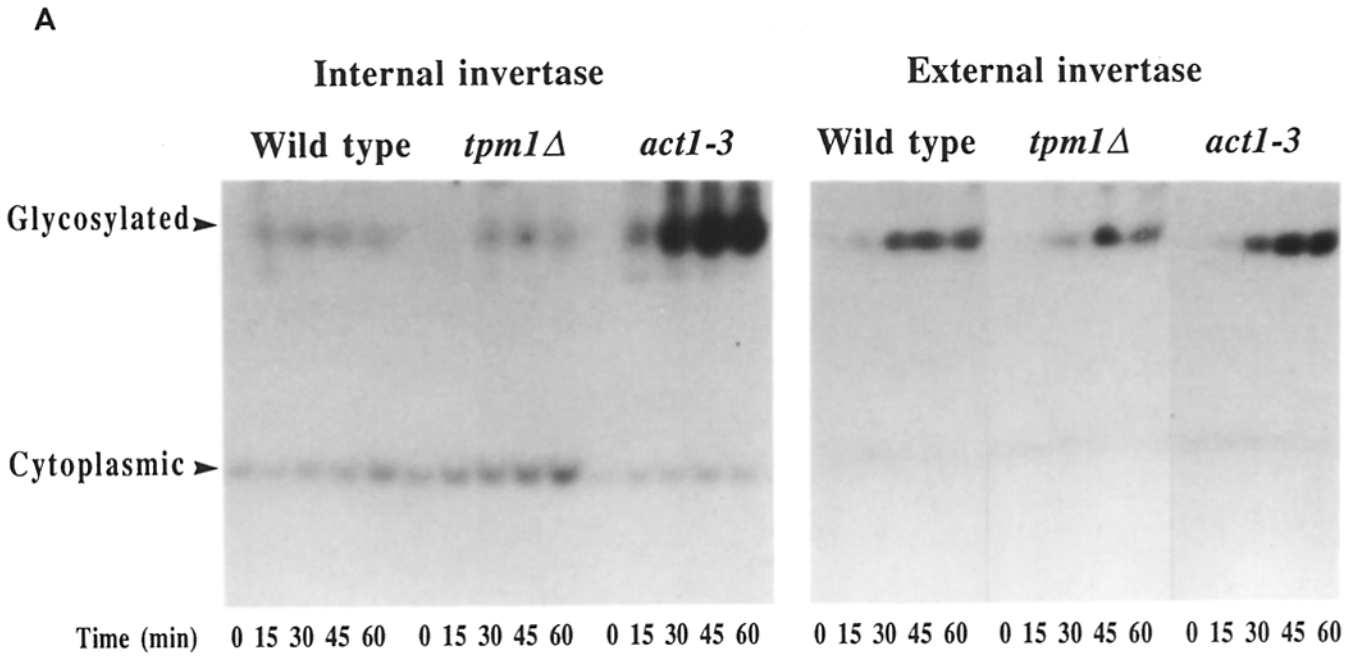

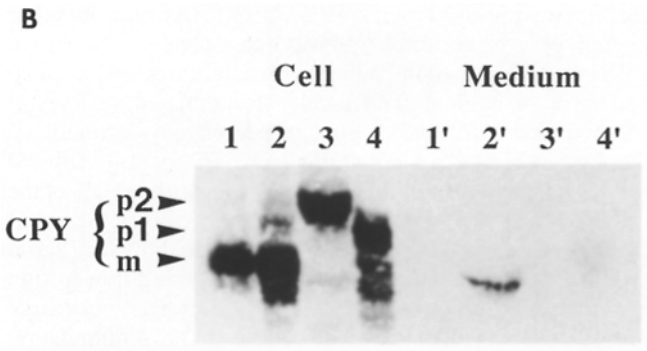

Figure 7. Invertase secretion and carboxypeptidase Y (CPY) delivery to the vacuole are normal in *tpm1Δ* cells. (*A*) Internal and external invertase. Wild-type (CUY25), *tpm1Δ* (ABY321) and *act1-3* (DBY2000) cells were grown to early log phase at room temperature and switched from 5% glucose to 0.1% glucose containing media to induce invertase secretion. Cytoplasmic and periplasmic invertase were assayed after fractionation on a native gel after 0, 15, 30, 45, and 60 min induction at 37°C. The fully glycosylated secretory form and the constitutively expressed nonglycosylated cytoplasmic form of invertase are indicated. (*B*) Delivery of CPY to the vacuole is normal in *tpm1Δ* cells. Wild-type (CUY25), *tpm1Δ* (ABY321), *pep4* (CGY339), and *sec18* (NY431) cells were grown at room temperature and the *pep4* and *sec18* cells shifted to 37°C for 2 h. All cells were grown in YEPD + 0.5% BSA to prevent proteolytic cleavage of the secreted CPY (Stevens et al., 1986). Total cell extracts and total proteins in the media were subjected to electrophoresis and immunoblotted with CPY antibodies. (Lane *1*) Wild type cells; (lane *2*) *tpm1Δ* cells; (lane *3*) *pep4* cells; (lane *4*) *sec18* cells. Lanes *1'–4'* are the media from the corresponding cells. The precursor *p1* and *p2* forms and mature (*m*) form of CPY are indicated.

a constitutively expressed transcript and a hexose repressed transcript (Carlson and Botstein, 1983). The product of the first transcript is nonglycosylated and remains soluble in the cytoplasm. The product of the repressible transcript becomes partially glycosylated in the endoplasmic reticulum and fully glycosylated in the Golgi apparatus. The fully glycosylated protein is packaged into vesicles that are transported to the bud, where the protein is released by exocytosis into the periplasmic space (Esmon et al., 1981). To look for defects in the secretory pathway, invertase was followed in wild-type cells, *tpm1Δ* cells and cells carrying the conditional *act1-3* mutation (Fig. 7 *A*). Cultures were grown overnight at the permissive temperature in repressing medium (containing 5% glucose), and then shifted into derepressing medium (0.1% glucose) at 37°C. Aliquots were harvested at various times and the proteins released after cell wall digestion (to liberate periplasmic invertase) and the proteins in spheroplasts (containing internal invertase) were fractionated on native gels and assayed for invertase activity. Invertase was inducible in all the strains and both the wild type and *tpm1Δ* cells secreted it to the periplasm. As reported (Novick and Botstein, 1985), the cells carrying the *act1-3* mutation secreted but also accumulated fully glycosylated invertase internally upon derepression. Under these conditions, no accumulation of internal glycosylated invertase in transit to the cell surface was seen in *tpm1Δ* cells.

Figure 6. Localization of a-agglutinin at the cell surface at various times after α-factor induction. Wild-type (CUY25) and *tpm1Δ* (ABY321) cells were grown to early log phase at room temperature and exposed to α-factor for the indicated times at both room temperature and 37°C. Cells were then fixed and stained for a-agglutinin by indirect immunofluorescence microscopy. (*A*) Wild type at room temperature; (*B*) *tpm1Δ* cells at room temperature; (*C*) wild-type cells at 37°C; (*D*) *tpm1Δ* cells at 37°C. Arrows indicate shmoo tips. Bar, 15 μm.

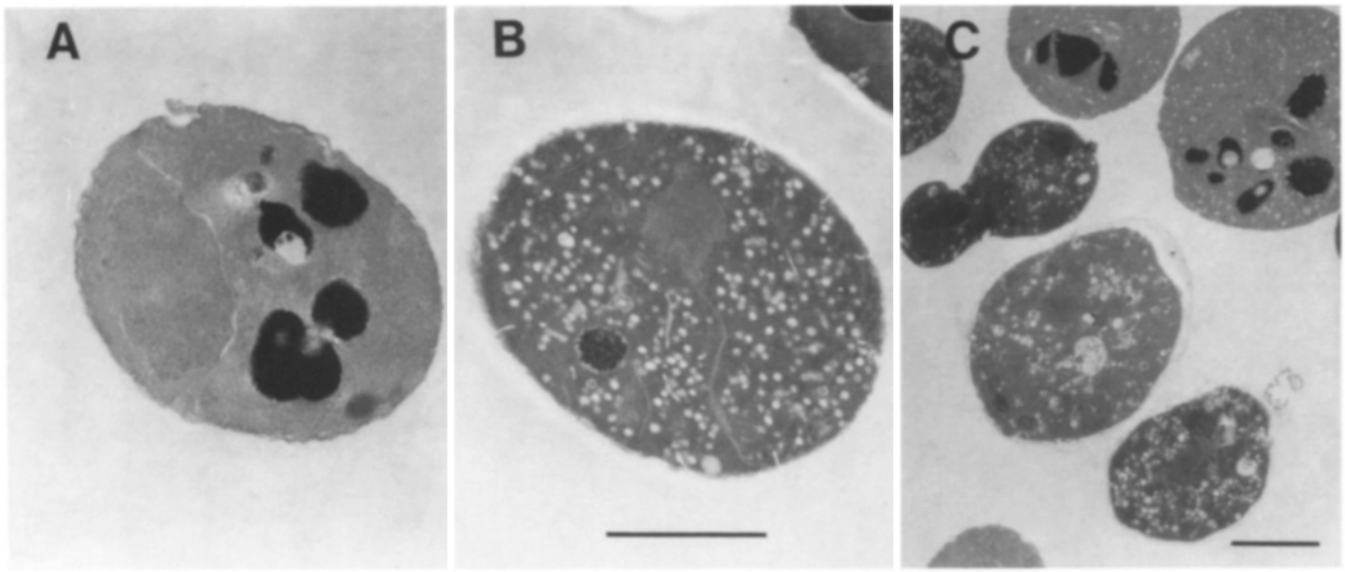

Figure 8. Electron micrographs of thin sections of wild-type (*A*) and *tpml*Δ cells (*B* and *C*). Wild-type (NY13) and *tpml*Δ cells (ABY411) were grown at room temperature and processed for EM. Bars, 1.5 μm.

It is possible that the secretion defect in the *tpml*Δ cells is minor and >1 h is necessary to result in any detectable accumulation. To explore this, cells were grown up in rich medium containing sucrose as carbon source for 20 h at 30°C and the internal and external levels of invertase were determined. Again, no greater accumulation of invertase could be detected in *tpml*Δ cells than in wild-type cells. Cells carrying conditional mutations in the *SEC4*, *SEC14*, or *SEC18* genes accumulated invertase after shifting to 37°C for 2 h (data not shown). These combined data imply that invertase secretion is not significantly impaired in *tpml*Δ cells.

CPY is an enzyme whose delivery to the vacuole can be monitored by changes in the apparent molecular weight of its precursors (Stevens et al., 1982). CPY is partially glycosylated in the ER to give a precursor designated pl, then fully glycosylated in the Golgi apparatus to give p2, and finally proteolytically cleaved in the vacuole by the *PEP4* gene product to yield mature CPY. To explore whether CPY is properly delivered to the vacuole in *tpml*Δ cells, blots of total proteins from wild-type cells, *tpml*Δ, *sec18*, and *pep4* cells were probed with antibody to CPY (Fig. 7 *B*). The CPY in the *tpml*Δ cells is essentially all in the mature form, indicating a normal vacuolar protein sorting pathway and a functional vacuole. Mutants defective in vacuolar protein sorting are unable to deliver CPY to the vacuole and, therefore, secrete it into the medium in the p2 form (Rothman and Stevens, 1986). A small amount of mature CPY is found in the medium of *tpml*Δ cells suggesting that this fully processed product is released into the medium probably by cell lysis because actin could also be detected by immunoblotting in the medium (data not shown).

Disruption of the TPM1 Gene Results in the Accumulation of Vesicles

Electron micrographs of thin section of *tpml*Δ cells revealed that they contained an abnormally large number of vesicles (Fig. 8). These resemble the secretory vesicles that accumulate in yeast cells conditionally defective in a late step of the secretory pathway (Novick et al., 1980). As with its other phenotypes, the accumulation was heterogeneous and varied with genetic background and growth conditions. Between 20 and 48% of haploid *tpml*Δ cells accumulated vesicles at room temperature and a greater percentage accumulated them when the cells were shifted to 37°C for 2 h. Diploid *tpml*Δ cells had a more severe phenotype, with ~60% of the cells grown at 30°C showing accumulated vesicles. Accumulation seemed to be correlated with cell size, but since serial sections have not been collected, a small cell in a thin section is not necessarily a small cell in reality. However, very large *tpml*Δ cells were packed with vesicles. The accumulation was not caused by the property of *tpml*Δ cells to yield ρ^- progenies at high frequency, as a similar fraction of ρ^- *tpml*Δ cells contained vesicles.

The accumulation of vesicles morphologically similar to late secretory vesicles appears to contradict the finding that *tpml*Δ cells do not accumulate internal invertase. To determine whether the vesicles are in fact intermediates in the secretory pathway, the membrane traffic of cells carrying both the *tpml*Δ disruption and conditional mutations in various *SEC* genes was examined. The *SEC* mutants have been classified into three major groups according to the membrane bound compartments that they accumulate at the restrictive temperature (Novick et al., 1980). Mutations in early genes (such as *SEC13*, *SEC18*) accumulate an exaggerated ER; mutations in genes involved in transport from the Golgi apparatus to the vacuole and to secretory vesicles (such as *SEC14*) develop an enlarged Golgi apparatus; and mutations in genes necessary for the exocytosis of secretory vesicles (such as *SEC1*, *SEC4*, and *SEC6*) accumulate secretory vesicles. If the *TPM1* gene product is involved in one or more steps in the secretory pathway, disruption of the *TPM1* gene in combination with a conditional *sec* mutation necessary for that step might be lethal. Such synthetic lethality between *sec* mutations has been very informative at identifying genes specifying interacting components of a particular step in the secretory pathway (for example see Salminen and Novick, 1987; Kaiser and Schekman, 1990). In addi-

Table IV. Organelle Accumulation in tpm1Δ sec Double Mutants

Relevant genotype (strain)	Accumulation at 23°C	Accumulation at 37°C*
Wild type (NY13)	None	None
tpm1Δ (ABY411)	Vesicles in 48% cells	Vesicles in 58% cells
tpm1Δ, sec13 (ABY415)	None	ER
tpm1Δ, sec18 (ABY416)	None	ER
tpm1Δ, sec14 (ABY413)	Vesicles in 14% cells	Golgi apparatus and some vesicles
tpm1Δ, sec1 (ABY409)	Vesicles in 49% cells	Vesicles in all cells
tpm1Δ, sec4 (ABY414)	Vesicles in 30% cells	Vesicles in all cells
tpm1Δ, sec6 (ABY412)	Vesicles in 40% cells	Vesicles in all cells

* Cells were shifted to 37°C for 2 h.

tion, if the vesicles seen in *tpm1Δ* cells are late secretory vesicles, a block at an early step of the pathway might be expected to reduce the accumulation of the late secretory vesicles. To explore double mutant combinations, the *TPM1* gene was disrupted in strains carrying the conditional mutations *sec1-1*, *sec4-8*, *sec6-4*, *sec13-1*, *sec14-3*, and *sec18-1*. No synthetic lethality was found among any of the double mutation combinations. In the *tpm1Δ* strains also harboring *sec1*, *sec4*, or *sec6* mutations, which affect a late step in the pathway, 30–50% of the cells accumulated vesicles when grown at room temperature (Table IV). Highly packed vesicles were seen in all the cells after shifting to 37°C due to the phenotypic expression of the conditional *sec* mutation (Fig. 9). The vesicles were indistinguishable from those accumulated at room temperature. In *tpm1Δ*, *sec14-3* cells, vesicles were found in ~14% of the cell population after growth at room temperature (Table IV and Fig. 9). This double mutant accumulated both Golgi apparatus and vesicles in most of the cells at 37°C. Since *TPM1⁺sec14-3* cells accumulate both Golgi apparatus and vesicles at 37°C, it is not clear if the vesicles seen in the *tpm1Δ*, *sec14-3* construct are a consequence of the *sec14-3* mutation or the *tpm1Δ* disruption. In contrast to the mutations affecting late steps in the secretory pathway, vesicles were rarely seen in the *tpm1Δ sec13-1* or *tpm1Δ sec18-1* mutants grown at room temperature (Table IV, Fig. 9). Our interpretation is that at the permissive temperature the mutations in these *SEC* genes reduce the flux through the pathway and so the defect that leads to late secretory vesicle accumulation is not seen. This supports the idea that the vesicles that accumulate in *tpm1Δ* are vesicular intermediates in the late secretory pathway.

Although the *sec13* and *sec18* mutations were able to phenotypically suppress the accumulation of vesicles seen in *tpm1Δ* cells, they did not suppress either the slower growth rate or the heterogeneous cell size (not shown).

Tpm1Δ and Myo2-66 Mutants Have Many Properties in Common and the Mutations Show Synthetic Lethality

Recently, Johnson et al. (1991) described the properties of a temperature-sensitive mutation, designated *myo2-66*, in a gene that encodes a myosin-like protein. The *myo2-66* mutants are in many ways similar to the *tpm1Δ* strain described here. This mutant was isolated from a screen after enriching for abnormally large cells (Prendergast et al., 1990) and arrests as unbudded cells at the restrictive temperature. At the restrictive temperature the *myo2-66* mutant has an aberrant actin cytoskeleton, has delocalized chitin deposition, and accumulates vesicles yet secretes invertase normally.

We have examined *myo2-66* mutant cells and found that they do not accumulate more invertase at their restrictive temperature than wild-type cells when grown in sucrose as the carbon source (data not shown). The a-agglutinin secretion pattern in the *myo2-66* cells was also similar to that in the *tpm1Δ* cells, normal at room temperature and slower and partially delocalized at 37° (data not shown). These similarities, together with the fact that tropomyosin and myosin are both important components of the contractile machinery of higher cells, prompted us to explore the phenotype of *tpm1Δ myo2-66* double mutants. A *tpm1Δ::URA3* strain was crossed to a *myo2-66ᵗˢ* strain. Sporulation of the resulting diploid gave no complete tetrads of four viable spores. Analysis of viable spores showed that no *tpm1Δ::URA3 myo2-66ᵗˢ* haploids were recovered in 12 sets of tetrads, suggesting that *tpm1Δ myo2-66* might be lethal. However, an excess lethality of *tpm1Δ* cells unrelated to *myo2-66* seemed to exist. To show the synthetic lethality more definitively, a *tpm1Δ::LEU2/TPM1⁺ myo2-66/MYO2⁺* diploid was transformed with a *TPM1/2μ(URA3)* plasmid before sporulation. Four viable spores were now recovered, with the temperature sensitivity (*myo2-66ᵗˢ*) segregating 2:2 and the Leu⁺ (*tpm1Δ*) segregating 2:2. The segregants were placed on FOA plates at room temperature to select for Ura⁻ cells that had lost the plasmid. Only the *tpm1Δ::LEU2 myo2-66ᵗˢ* segregants were unable to loose the *TPM1/2μ(URA3)* plasmid. Since the *myo2-66* mutant grows well under these conditions, we conclude that the *tpm1Δ myo2-66* double mutant is inviable at room temperature.

Discussion

Tropomyosin is an important microfilament-associated protein of cells from mammals to yeast, yet outside of striated muscle its function is not clearly understood. The availability of yeast mutants that lack tropomyosin allows an assessment of its function in at least this organism. We have shown that cells in which the *TPM1* gene was functionally deleted had no detectable actin cables. This, and the finding of an association of tropomyosin with actin filaments in vitro and in vivo, led to the idea that tropomyosin is involved in the assembly or stabilization of actin cables in yeast (Liu and Bretscher, 1989*b*).

Cells lacking a functional *TPM1* gene grow remarkably well despite their aberrant actin cytoskeleton. The lack of

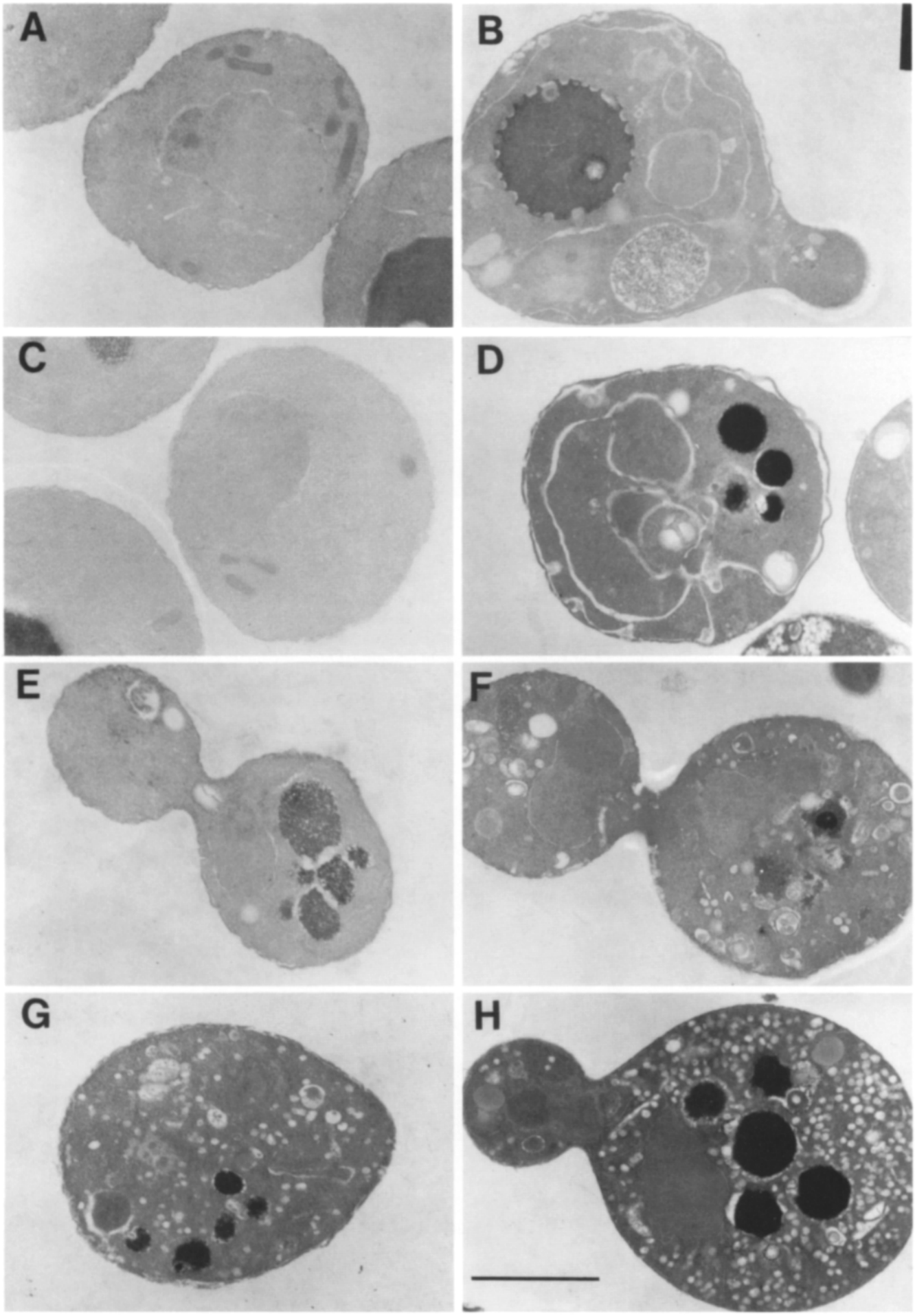
A
B
C
D
E
F
G
H

tropomyosin imparts considerable heterogeneity into the population, with the larger cells having a more abnormal phenotype than the smaller cells, making a phenotypic characterization all the more difficult. Despite this difficulty, there appears to be a common thread that links all the results: cells lacking tropomyosin have a partial defect in the directed transport of components to their correct destination on the cell surface. The fact that the abnormal phenotype is more severe in larger cells, which are still viable, argues strongly for a partial defect in some form of intracellular transport.

In exponentially growing wild-type cells, all the growth is directed to the bud and the mother cell maintains a constant size during the cell cycle. In *tpm1Δ* cells, the growth is less directed and both the mother and daughter cells grow. This results in smaller than normal daughter cells and larger than normal mother cells. The defect in directed transport appears to be more pronounced in *tpm1Δ* diploids than haploids since they show greater heterogeneity in cell size, presumably because their larger size makes the greater distance that materials have to be transported more critical.

Abnormalities in chitin deposition in *tpm1Δ* cells also seem to be size dependent, with smaller cells having a relatively normal staining pattern, and larger cells having more delocalized staining. The phenotype is more severe at 37°C with most of the cells having completely delocalized chitin. However, since the mechanism of chitin deposition is unknown, it is hard to evaluate the reason for chitin mislocalization in the *tpm1Δ* cells.

Perhaps the clearest physiological demonstration that the *tpm1Δ* cells are partially defective in directed secretion are our results examining the transit time and localization of a-agglutinin at 37°C. The transit time for a-agglutinin to reach the cell surface after induction is at least two times longer than in isogenic wild-type cells, and when it does come to the surface, some of it is inappropriately localized. However, the targeting of a-agglutinin looks perfectly normal at room temperature and most of it is localized in the bud even at 37°C. This mislocalization phenotype is not as strong as expected if the directed transport of secretory vesicles, presumably along actin cables, is the only mechanism for polarized cell surface growth. It is therefore very likely that there are also proteins specifically localized at sites of active surface growth that facilitate the fusion of the secretory vesicles with the plasma membrane. The absence of these proteins in the mother cell would make exocytosis inefficient and be expected to lead to the accumulation of vesicles in the mother cell. Conditional mutations affecting targeting proteins of this type might confer a defect in bud formation, and arrest as unusually large unbudded cells at the restrictive temperature, such as is found for the *CDC24, CDC42, CDC43,* and *BEM1* gene (Sloat et al., 1981; Adams et al., 1990; Bender and Pringle, 1991). The targeting of the secretory protein acid phosphatase in *cdc24* mutant cells has been shown to be completely delocalized (Field and Schekman, 1980).

This same problem appears to afflict the mating response of *tpm1Δ* cells. When wild-type cells of opposite mating types are mixed, cells grow towards each other forming shmoo projections. Agglutinin is targeted to the shmooing tip that sticks cells of opposite mating types together. During this process, actin cables are oriented towards the shmoo tip. If this morphological change does not occur correctly, as in the case of *tpm1Δ* cells which do not assemble actin cables directed to the tip, the cells cannot conjugate efficiently. It is not yet clear why *tpm1Δ* cells require more mating pheromone to induce shmoo formation; they seem to be about as sensitive as wild-type cells to α-factor induced growth inhibition as determined by a halo assay. In the next step of zygote formation, removal of the cell wall between the two conjugating cells involves the correct targeting of the cell wall lysis and fusogenic materials; this too seems to be partially defective in *tpm1Δ* cells.

Electron microscopy reveals that many of the cells in an exponentially growing population of the *tpm1Δ* mutant have an abnormal accumulation of vesicles, with a greater percentage of diploids than haploids showing this phenotype. These are reminiscent of the vesicles that accumulate in mutants blocked late in the secretory pathway. We have results to suggest that these vesicles are in the late secretory pathway. A combination of the *tpm1Δ* mutation with conditional mutations in genes required for late steps in the secretory pathway have an "additive" phenotype. That is, at the permissive temperature the cells are viable but many of them accumulate vesicles due to the *tpm1Δ* mutation. At the restrictive temperature all the cells accumulate vesicles due to both mutations. In contrast, combinations of the *tpm1Δ* mutation with either *sec13-1* or *sec18-1* show the phenotype of the *sec* mutant. At the permissive temperature, the cells are free of internal vesicles, whereas at the restrictive temperature they show the phenotype typical of their conditional mutation. These two genes have their earliest point of action in the secretory pathway between the endoplasmic reticulum and the Golgi apparatus (Kaiser and Schekman, 1990). Conditional mutations in these genes will presumably slow the flux through the secretory pathway even at the permissive temperature. Since they suppress the formation of vesicles by the *tpm1Δ* mutation, they presumably lie upstream of the partial defect imposed by the loss of tropomyosin. This places the site of action sensitive to the lack of tropomyosin as post-Golgi apparatus.

The phenotype of cells carrying the *myo2-66* mutation is remarkably similar to *tpm1Δ* cells. Moreover, the *myo2-66* and *tpm1Δ* mutations show synthetic lethality, strongly implicating their wild-type products as two interacting components of an important function. Very recently, Govindan et al. (1991) reported that *myo2-66* shows synthetic lethality with mutations in a subset of late acting *SEC* genes (*sec2, sec4, sec5, sec8, sec9, sec10* and *sec15*) and that duplicating *SEC4* can partially suppress the phenotype of the *myo2-66* mutant. This seems to imply that the *MYO2* gene product

Figure 9. Ultrastructure of stains carrying both *tpm1Δ* and a *sec* mutation. Double mutants were grown at room temperature to ~5 × 10^6 cells/ml and half the culture shifted to 37°C for 2 h. Cells were then processed for the preparation of thin section and examination by electron microscopy. *A, C, E,* and *G* are cells grown at room temperature. *B, D, F,* and *H* are cells after 2 h at 37°C. (*A* and *B*) *sec13tpm1Δ* cells (ABY415); (*C* and *D*) *sec18tpm1Δ* cells (ABY 416); (*E* and *F*) *sec14tpm1Δ* cells (ABY413); and (*G* and *H*) *sec1tpm1Δ* cells (ABY409). Bar, 1.5 μm.

acts in the late secretory pathway. The results presented here also imply that the *TPM1* gene product may participate in this part of the pathway.

Despite this evidence for a defect in the late secretion pathway, there is no abnormally large accumulation of invertase found in either *tpm1Δ* or *myo2-66* cells. If the products of the *MYO2* and *TPM1* genes are involved in vesicle transport and defects in them lead to the accumulation of secretory vesicles, biochemical intermediates in the pathway should also accumulate. Indeed, given the number of vesicles seen, particularly in the *tpm1Δ* cells, a very significant accumulation should have been found, yet none was. This paradox is not easy to resolve, and we have no completely satisfactory explanation. One possibility is that secretory vesicles only accumulate slowly and if they do not fuse with their target membrane their contents become degraded. Another possibility is that *MYO2*, *TPM1*, and some of the late *SEC* gene products are necessary for a vesicular transport step in another pathway and that the accumulated vesicles are intermediates in this pathway. For example, there may be two parallel secretory pathways from the Golgi apparatus to the plasma membrane, both requiring the late *sec* genes, but only one requiring the *MYO2* and *TPM1* gene products: this would be the route not carrying invertase. Alternatively, since many of the late, and some of the early, *SEC* genes are involved in endocytosis (Riezman, 1985), the accumulated vesicles may be intermediates in this pathway, although preliminary uptake studies with lucifer yellow CH do not support this possibility. Characterization of the vesicles that accumulate in *tpm1Δ* cells will help resolve this puzzle.

The results presented in this paper support a role for actin cables in vesicular transport and cell wall growth. This suggestion was first put forth by Kilmartin and Adams (1984), and Adams and Pringle (1984). It has consistently been supported by observations on the analysis of genes for many actin binding proteins (see introduction) and the analysis of the *myo2-66* mutation described above. Support has also come from another direction. Novick et al. (1989) isolated allele-specific suppressors of the *act1-1* mutation that led to the identification of five genes (designated *SAC1* to *SAC5*) that may encode actin-binding proteins. Suppressors of a mutation in the *SEC14* gene, which is necessary for transport from the Golgi to both the vacuole and secretory vesicles (Novick et al., 1981) and encodes a phospholipid transfer protein (Bankaitis et al., 1990), were also found to lie in the *SAC1* gene (Cleves et al., 1989). The *sac1* alleles that suppressed the *sec14* mutations also suppressed the *act1-1* mutation. Additionally, the *sac1* mutations could also partially suppress some *sec6* and *sec9* mutations, and showed synthetic lethality with *sec13* and *sec20* mutations. The simple view of these studies is that the *sac1* mutations can suppress mutations in genes needed after the Golgi apparatus in the secretory pathway, whereas the same *sac1* mutations aggravate defects early in the pathway (ER to Golgi apparatus). Whatever the mechanism, these results again provide genetic evidence for a functional link between the actin cytoskeleton and the secretory pathway.

Despite these clear links to the secretory pathway, it should be noted that cells harboring mutations in actin-binding proteins have a more complicated phenotype than *sec* mutants. It appears that mutants such as *tpm1Δ* cells are also partially defective in delivering the secretory products to their correct destinations, which leads to a defect in morphogenesis, and may be defective in other functions yet to be appreciated. Only when appropriate mutations that affect specific aspects of microfilament function are available will it really become possible to pinpoint the precise function of microfilaments in vital processes.

We are very grateful to Matthew Footer for help with the photography; to T. Stevens and W. Tanner for antibodies to CPY and a-agglutinin, respectively; to G. Johnston, T. Huffaker, and P. Novick for strains; and to Bill Brown and our lab colleagues for comments on the manuscript.

This work was funded by grant GM39066 from the National Institutes of Health.

Received for publication 6 February 1992 and in revised form 15 April 1992.

References

Adams, A. E. M., and D. Botstein. 1989. Dominant suppressors of yeast actin mutations that are reciprocally suppressed. *Genetics*. 121:675–683.

Adams, A. E. M., and J. R. Pringle. 1984. Relationship of actin and tubulin distribution to bud growth in wild-type and morphogenetic mutant *Saccharomyces cerevisiae*. *J. Cell Biol.* 98:934–945.

Adams, A. E. M., D. Botstein, and D. G. Drubin. 1989. A yeast actin-binding protein is encoded by *SAC6*, a gene found by suppression of an actin mutation. *Science (Wash. DC)*. 243:231–233.

Adams, A. E. M., D. I. Johnson, R. M. Longnecker, B. F. Sloat, and J. R. Pringle. 1990. *CDC42* and *CDC43*, two additional genes involved in budding and the establishment of cell polarity in the yeast *Saccharomyces cerevisiae*. *J. Cell Biol.* 111:131–142.

Adams, A. E. M., D. Botstein, and D. G. Drubin. 1991. Requirement of yeast fimbrin for actin organization and morphogenesis in vivo. *Nature (Lond.)*. 354:404–408.

Amatruda, J. F., J. F. Cannon, K. Tatchell, C. Hug, and J. A. Cooper. 1990. Disruption of the actin cytoskeleton in yeast capping protein mutants. *Nature (Lond.)*. 344:352–354.

Bankaitis, V. A., J. F. Aitken, A. E. Cleves, and W. Dowhan. 1990. An essential role for a phospholipid transfer protein in yeast Golgi function. *Nature (Lond.)*. 347:561–562.

Barnes, G., D. G. Drubin, and T. Stearns. 1990. The cytoskeleton of *Saccharomyces cerevisiae*. *Curr. Opinion Cell Biol.* 2:109–115.

Bender, A. and J. R. Pringle. 1991. Use of a screen for synthetic lethal and multicopy suppressee mutants to identify two new genes involved in morphogenesis in *Saccharomyces cerevisiae*. *Mol. Cell Biol.* 11:1295–1305.

Carlson, M., and D. Botstein. 1982. Two differentially regulated mRNAs with different 5′ ends encode secreted and intracellular forms of yeast invertase. *Cell*. 28:145–154.

Cleves, A. E., P. J. Novick, and V. A. Bankaitis. 1989. Mutations in the *SAC1* gene suppress defects in yeast Golgi and yeast actin function. *J. Cell Biol.* 109:2939–2950.

Cummins, P., and S. V. Perry. 1974. Chemical and immunological characteristics of tropomyosins from striated and smooth muscle. *Biochem. J.* 141:43–49.

Drubin, D. G., K. G. Miller, and D. Botstein. 1988. Yeast actin-binding proteins: evidence for a role in morphogenesis. *J. Cell Biol.* 107:2551–2561.

Drubin, D. G., J. Mulholland, Z. M. Zhu, and D. Botstein. 1990. Homology of a yeast actin-binding protein to signal transduction proteins and myosin-I. *Nature (Lond.)*. 343:388–390.

Dutcher, S. K., and L. H. Hartwell. 1983. Genes that act before conjugation to prepare the *Saccharomyces cerevisiae* nucleus for caryogamy. *Cell*. 33:203–210.

Ebashi, S., M. Endo, and I. Ohtsuki. 1969. Control of muscle contractions. *Quant. Rev. Biophys.* 2:351–384.

Field, C., and R. Schekman. 1980. Localized secretion of acid phosphatase reflects the pattern of cell surface growth in *Saccharomyces cerevisiae*. *J. Cell Biol.* 86:123–128.

Gabriel, O., and S. Wang. 1969. Determination of enzymatic activity in polyacrylamide gels. *Anal. Biochem.* 27:515–554.

Gallwitz, D., and I. Sures. 1980. Structure of a split yeast gene: complete nucleotide sequence of the actin gene in Saccharomyces cerevisiae. *Proc. Natl. Acad. Sci. USA*. 77:2546–2550.

Govindan, B., R. Bowser, and P. Novick. 1991. Role of the unconventional myosin gene *MYO2* in the yeast secretory pathway. *J. Cell Biol.* 115:185a.

Haarer, B. K., S. H. Lillie, A. E. M. Adams, V. Magdolen, W. Bandlow, and S. S. Brown. 1990. Purification of profilin from *Saccharomyces cerevisiae* and analysis of profilin-deficient cells. *J. Cell Biol.* 100:105–114.

Hasek, J., I. Rupes, J. Svobodova, and E. Streiblova. 1987. Tubulin and actin topology during zygote formation of *Saccharomyces cerevisiae*. *J. Gen. Microbiol.* 133:3355–3363.

Hill, J. E., A. M. Myers, T. J. Koerner, and A. Tzagoloff. 1986. Yeast/E. coli shuttle vectors with multiple unique restriction sites. *Yeast.* 21:163–167.

Huffaker, T. C., and A. Bretscher. 1991. Strategies for cloning and analyzing genes encoding cytoskeletal proteins in the yeast *Saccharomyces cerevisiae*. In Molecular Motors and the Cytoskeleton. R. Vallee, editor. *Methods Enzymol.* 196:355–368.

Huffaker, T. C., M. A. Hoyt, and D. Botstein. 1987. Genetic analysis of the yeast cytoskeleton. *Annu. Rev. Genet.* 21:259–284.

Ito, H., Y. Jukuda, K. Murata, and A. Kimura. 1983. Transformation of intact yeast cells treated with alkali cations. *J. Bacteriol.* 153:163–168.

Johnston, G. C., J. A. Prendergast, and R. A. Singer. 1991. The Saccharomyces cerevisiae *MYO2* gene encodes an essential myosin for vectorial transport of vesicles. *J. Cell Biol.* 113:539–551.

Kaiser, C. A., and R. Schekman. 1990. Distinct sets of *SEC* genes govern transport vesicle formation and fusion early in the secretory pathway. *Cell.* 61:723–733.

Karlick, C. C., and E. A. Fyrberg. 1986. Two Drosophila melanogaster tropomyosin genes: structure and functional aspects. *Mol. Cell. Biol.* 6:1965–1973.

Kilmartin, J., and A. E. M. Adams. 1984. Structural rearrangements of tubulin and actin during the cell cycle of the yeast *Saccharomyces*. *J. Cell Biol.* 98:922–933.

Leesmiller, J. P., and D. M. Helfman. 1991. The Molecular Basis for Tropomyosin Isoform Diversity. *Bioessays.* 13:429–437.

Liu, H., and A. Bretscher. 1989*a*. Purification of tropomyosin from *Saccharomyces cerevisiae* and identification of related proteins in *Schizosaccharomyces* and *Physarum*. *Proc. Natl. Acad. Sci. USA.* 86:90–93.

Liu, H., and A. Bretscher. 1989*b*. Disruption of the single tropomyosin gene in yeast results in the disappearance of actin cables from the cytoskeleton. *Cell.* 57:233–242.

Magdolen, V., U. Oechsner, G. Muller, and W. Bandlow. 1988. The intron containing gene for yeast profilin (PFY) encodes a vital function. *Mol. Cell Biol.* 8:5108–5115.

Novick, P., and D. Botstein. 1985. Phenotypic analysis of temperature-sensitive yeast actin mutants. *Cell.* 40:405–416.

Novick, P., C. Field, and R. Schekman. 1980. Identification for 23 complementation groups required for post-translational events in the yeast secretory pathway. *Cell.* 25:205–215.

Novick, P., B. C. Osmond, and D. Botstein. 1989. Suppressors of yeast actin mutations. *Genetics.* 121:659–674.

Ng, R., and J. Abelson. 1980. Isolation and sequence for the gene for actin in *Saccharomyces cerevisiae*. *Proc. Natl. Acad. Sci. USA.* 77:3912–3916.

Prendergast, J. P., L. E. Murray, A. R. Rowley, D. R. Carruthers, R. A. Singer, and G. C. Johnston. 1990. Size selection identifies new genes that regulate *Saccharomyces cerevisiae* cell proliferation. *Genetics.* 124:81–90.

Riezman, H. 1985. Endocytosis in yeast: several of the yeast secretory mutants are defective in endocytosis. *Cell.* 40:1001–1009.

Rothman, J., and T. H. Stevens. 1986. Protein sorting in yeast: mutants defective in vacuole biogenesis mislocalize vacuolar proteins into the late secretory pathway. *Cell.* 47:1041–1051.

Salminen, A., and P. J. Novick. 1987. A ras-like protein is required for a post-Golgi event in yeast secretion. *Cell.* 49:527–538.

Sherman, F., G. R. Fink, and C. Lawrence. 1974. Methods in yeast genetics. Cold Spring Harbor Laboratory, Cold Spring Harbor, NY.

Shortle, D., J. E. Haber, and D. Botstein. 1982. Lethal disruption of the yeast actin gene by integrative DNA transformation. *Science (Wash. DC).* 217:371–373.

Shortle, D., P. Novick, and D. Botstein. 1984. Construction and genetic characterization of temperature-sensitive mutant alleles of the yeast actin gene. *Proc. Natl. Acad. Sci. USA.* 81:4889–4893.

Sloat, B. F., and J. R. Pringle. 1978. A mutant of yeast defective in cellular morphogenesis. *Science (Wash. DC).* 200:1171–1173.

Sloat, B. F., A. Adams, and J. R. Pringle. 1981. Roles of the *CDC24* gene product in cellular morphogenesis during the *Saccharomyces cerevisiae* cell cycle. *J. Cell Biol.* 89:395–405.

Solomon, F. 1991. Analyses of the cytoskeleton in *Saccharomyces cerevisiae*. *Annu. Rev. Cell Biol.* 7:633–662.

Stevens, T., B. Esmon, and R. Schekman. 1982. Early stages in the yeast secretory pathway are required for transport of carboxypeptidase Y to the vacuole. *Cell.* 30:439–448.

Stevens, T. H., J. H. Rothman, G. S. Payne, and R. Schekman. 1986. Gene dosage-dependent secretion of yeast vacuolar carboxypeptidase Y. *J. Cell Biol.* 102:1551–1557.

Trueheart, J., J. D. Boeke, and G. R. Fink. 1987. Two genes required for cell fusion during yeast conjugation: evidence for a pheromone-induced surface protein. *Mol. Cell Biol.* 7:2316–2328.

Walworth, N. C., and P. J. Novick. 1987. Purification and characterization of constitutive secretory vesicles from yeast. *J. Cell Biol.* 105:163–174.

Watts, F. Z., D. M. Miller, and E. Orr. 1985. Identification of myosin heavy chain in *Saccharomyces cerevisiae*. *Nature (Lond.).* 316:83–85.

Watts, F. Z., G. Shiels, and E. Orr. 1987. The yeast MYO1 gene encoding a myosin-like protein required for cell division. *EMBO (Eur. Mol. Biol. Organ.) J.* 6:3499–3505.

Watzele, M., F. Klis, and W. Tanner. 1988. Purification and characterization of the inducible a-agglutinin of *Saccharomyces cerevisiae*. *EMBO (Eur. Mol. Biol. Organ.) J.* 7:1483–1488.